Supporting Information

Water Stability Studies of Hybrid Iodoargentates Containing N-Alkylated or N-Protonated Structure Directing Agents: Exploring Noncentrosymmetric Hybrid Structures

Guang-Ning Liu,*[,a,b], Xiao-Ming Jiang,[b] Qing-Shun Fan,[a] Muhammad Bilal Hussain,[a] Ke Li,[a] Hui Sun,[a] Xin-Yu Li,[a] Zhen-Wei Zhang [a] and Cuncheng Li*[,a]

[a]*Key Laboratory of Chemical Sensing & Analysis in Universities of Shandong, School of Chemistry and Chemical Engineering, University of Jinan, Jinan, Shandong 250022, P. R. China*

[b]*State Key Laboratory of Structural Chemistry, Fujian Institute of Research on the Structure of Matter, Chinese Academy of Sciences, Fuzhou, Fujian 350002, P. R. China*

Table S1. Selected Bond Distances (Å) and Angles (°) for **1**–**4**.

1			
Bond	(Å)	Bond	(Å)
Ag(1)-I(3)	2.825(1)	N(2)-C(18)	1.397(4)
Ag(1)-I(1)	2.854(1)	N(2)-C(11)	1.459(4)
Ag(1)-I(2)	2.883(1)	C(1)-C(2)	1.440(8)
Ag(1)-I(4)	2.902(1)	C(4)-C(5)	1.380(6)
I(1)-Ag(1)#1	2.854(1)	C(4)-C(9)	1.415(6)
I(2)-Ag(1)#1	2.883(1)	C(5)-C(6)	1.256(7)
I(3)-Ag(1)#2	2.825(1)	C(6)-C(7)	1.274(9)
I(4)-Ag(1)#2	2.902(1)	C(7)-C(8)	1.436(10)
S(1)-C(3)	1.678(5)	C(8)-C(9)	1.396(7)
S(1)-C(9)	1.717(5)	C(10)-C(11)	1.516(5)
S(2)-C(12)	1.689(4)	C(13)-C(14)	1.375(5)
S(2)-C(13)	1.733(3)	C(13)-C(18)	1.428(5)
N(1)-C(3)	1.299(6)	C(14)-C(15)	1.337(5)

N(1)-C(4)	1.391(6)	C(15)-C(16)	1.377(5)
N(1)-C(2)	1.464(6)	C(16)-C(17)	1.360(5)
N(2)-C(12)	1.274(4)	C(17)-C(18)	1.376(4)
Angle	(°)	Angle	(°)
I(3)-Ag(1)-I(1)	110.81(1)	C(5)-C(4)-C(9)	121.8(4)
I(3)-Ag(1)-I(2)	120.05(1)	N(1)-C(4)-C(9)	107.6(4)
I(1)-Ag(1)-I(2)	104.65(1)	C(6)-C(5)-C(4)	116.6(5)
I(3)-Ag(1)-I(4)	107.37(1)	C(5)-C(6)-C(7)	129.4(7)
I(1)-Ag(1)-I(4)	107.99(1)	C(6)-C(7)-C(8)	118.0(6)
I(2)-Ag(1)-I(4)	105.37(1)	C(9)-C(8)-C(7)	117.9(5)
Ag(1)-I(1)-Ag(1)#1	75.01(1)	C(8)-C(9)-C(4)	116.3(4)
Ag(1)#1-I(2)-Ag(1)	74.12(1)	C(8)-C(9)-S(1)	131.0(4)
Ag(1)#2-I(3)-Ag(1)	73.61(1)	C(4)-C(9)-S(1)	112.7(3)
Ag(1)-I(4)-Ag(1)#2	71.36(1)	N(2)-C(11)-C(10)	115.0(3)
C(3)-S(1)-C(9)	89.4(2)	N(2)-C(12)-S(2)	115.8(3)
C(12)-S(2)-C(13)	89.98(16)	C(14)-C(13)-C(18)	119.4(3)
C(3)-N(1)-C(4)	115.7(4)	C(14)-C(13)-S(2)	130.8(3)
C(3)-N(1)-C(2)	133.9(4)	C(18)-C(13)-S(2)	109.8(2)
C(4)-N(1)-C(2)	110.4(4)	C(15)-C(14)-C(13)	118.0(3)
C(12)-N(2)-C(18)	114.1(3)	C(14)-C(15)-C(16)	122.4(3)
C(12)-N(2)-C(11)	126.5(3)	C(17)-C(16)-C(15)	122.6(3)
C(18)-N(2)-C(11)	119.4(2)	C(16)-C(17)-C(18)	115.9(3)
C(1)-C(2)-N(1)	110.0(5)	C(17)-C(18)-N(2)	128.0(3)
N(1)-C(3)-S(1)	114.6(4)	C(17)-C(18)-C(13)	121.7(3)
C(5)-C(4)-N(1)	130.6(4)	N(2)-C(18)-C(13)	110.3(2)

Symmetry transformations used to generate equivalent atoms: #1 -x-1, y, z; #2 -x, y, z.

2

Bond	(Å)	Bond	(Å)
Ag(1)-I(1)#1	2.917(1)	S(1)-C(7)	1.678(5)
Ag(1)-I(1)#2	2.917(1)	S(1)-C(1)	1.738(4)
Ag(1)-I(1)	2.917(1)	N(1)-C(7)	1.316(5)
Ag(1)-I(1)#3	2.917(1)	N(1)-C(6)	1.397(5)
Ag(2)-I(1)#4	2.883(1)	N(1)-C(8)	1.482(5)
Ag(2)-I(1)	2.883(1)	C(1)-C(2)	1.394(6)
Ag(2)-I(1)#5	2.883(1)	C(1)-C(6)	1.398(6)
Ag(2)-I(1)#2	2.883(1)	C(2)-C(3)	1.377(6)
Ag(3)-I(2)#6	2.863(1)	C(3)-C(4)	1.388(6)
Ag(3)-I(2)#7	2.863(1)	C(4)-C(5)	1.382(6)
Ag(3)-I(2)#8	2.864(1)	C(5)-C(6)	1.390(6)
Ag(3)-I(2)	2.864(1)	C(8)-C(9)	1.505(7)
I(2)-Ag(3)#9	2.863(1)	C(9)-C(10)	1.484(8)

Angle	(°)	Angle	(°)
I(1)#1-Ag(1)-I(1)#2	115.13(1)	Ag(3)#9-I(2)-Ag(3)	81.80(2)
I(1)#1-Ag(1)-I(1)	115.13(1)	C(7)-S(1)-C(1)	90.1(2)
I(1)#2-Ag(1)-I(1)	98.66 (2)	C(7)-N(1)-C(6)	112.7(4)
I(1)#1-Ag(1)-I(1)#3	98.66(2)	C(7)-N(1)-C(8)	122.7(4)
I(1)#2-Ag(1)-I(1)#3	115.13(1)	C(6)-N(1)-C(8)	124.6(4)
I(1)-Ag(1)-I(1)#3	115.13(1)	C(2)-C(1)-C(6)	121.5(4)
I(1)#4-Ag(2)-I(1)	114.28(1)	C(2)-C(1)-S(1)	128.1(4)
I(1)#4-Ag(2)-I(1)#5	100.24(2)	C(6)-C(1)-S(1)	110.4(3)
I(1)-Ag(2)-I(1)#5	114.28(1)	C(3)-C(2)-C(1)	116.9(4)
I(1)#4-Ag(2)-I(1)#2	114.28(1)	C(2)-C(3)-C(4)	121.7(4)
I(1)-Ag(2)-I(1)#2	100.24(2)	C(5)-C(4)-C(3)	122.0(4)
I(1)#5-Ag(2)-I(1)#2	114.28(1)	C(4)-C(5)-C(6)	116.9(4)
I(2)#6-Ag(3)-I(2)#7	98.21(2)	C(5)-C(6)-N(1)	127.4(4)

I(2)#6-Ag(3)-I(2)#8	115.38(1)	C(5)-C(6)-C(1)	121.0(4)
I(2)#7-Ag(3)-I(2)#8	115.38(1)	N(1)-C(6)-C(1)	111.5(4)
I(2)#6-Ag(3)-I(2)	115.38(1)	N(1)-C(7)-S(1)	115.3(3)
I(2)#7-Ag(3)-I(2)	115.38(1)	N(1)-C(8)-C(9)	112.7(4)
I(2)#8-Ag(3)-I(2)	98.19(2)	C(10)-C(9)-C(8)	113.2(5)
Ag(2)-I(1)-Ag(1)	80.55(2)		

Symmetry transformations used to generate equivalent atoms: #1 y, -x+1/2, -z+1/2; #2 -x+1/2, -y+1/2, z; #3 -y+1/2, x, -z+1/2; #4 -y+1/2, x, -z-1/2; #5 y, -x+1/2, -z-1/2; #6 y-1/2, -x+1, z+1/2; #7 -y+1, x+1/2, z+1/2; #8 -x+1/2, -y+3/2, z; #9 -y+1, x+1/2, z-1/2.

3

Bond	(Å)	Bond	(Å)
Ag(1)-I(2)#1	2.807(1)	N(1)-C(7)	1.294(6)
Ag(1)-I(2)	2.840(1)	N(1)-C(6)	1.384(5)
Ag(1)-I(1)	2.889(1)	C(1)-C(2)	1.378(6)
Ag(1)-I(1)#1	2.921(1)	C(1)-C(6)	1.400(5)
I(1)-Ag(1)#2	2.921(1)	C(2)-C(3)	1.361(7)
I(2)-Ag(1)#2	2.807(1)	C(3)-C(4)	1.389(7)
S(1)-C(7)	1.674(5)	C(4)-C(5)	1.362(6)
S(1)-C(1)	1.743(4)	C(5)-C(6)	1.380(5)
Angle	(°)	Angle	(°)
I(2)#1-Ag(1)-I(2)	127.88(2)	C(2)-C(1)-S(1)	129.4(3)
I(2)#1-Ag(1)-I(1)	114.28(2)	C(6)-C(1)-S(1)	109.6(3)
I(2)-Ag(1)-I(1)	97.92(1)	C(3)-C(2)-C(1)	116.8(4)
I(2)#1-Ag(1)-I(1)#1	97.93(1)	C(2)-C(3)-C(4)	123.0(4)
I(2)-Ag(1)-I(1)#1	106.17(2)	C(5)-C(4)-C(3)	120.2(4)
I(1)-Ag(1)-I(1)#1	112.80(2)	C(4)-C(5)-C(6)	118.2(4)
Ag(1)-I(1)-Ag(1)#2	80.12(1)	C(5)-C(6)-N(1)	128.4(4)

Ag(1)#2-I(2)-Ag(1)	82.93(1)	C(5)-C(6)-C(1)	120.8(4)
C(7)-S(1)-C(1)	90.4(2)	N(1)-C(6)-C(1)	110.9(3)
C(7)-N(1)-C(6)	114.6(4)	N(1)-C(7)-S(1)	114.4(4)
C(2)-C(1)-C(6)	121.0(4)		

Symmetry transformations used to generate equivalent atoms: #1 x, -y+3/2, z-1/2; #2 x, -y+3/2, z+1/2.

4

Bond	(Å)	Bond	(Å)
Ag(1)-I(2)	2.786(1)	S(1)-C(7)	1.692(3)
Ag(1)-I(3)#1	2.854(1)	S(1)-C(1)	1.742(3)
Ag(1)-I(3)	2.894(1)	N(1)-C(7)	1.362(4)
Ag(1)-I(1)	2.911(1)	N(1)-C(6)	1.413(4)
Ag(1)-Ag(2)	3.057(1)	N(2)-C(7)	1.320(4)
Ag(2)-I(2)	2.783(1)	C(1)-C(6)	1.401(4)
Ag(2)-I(1)#2	2.848(1)	C(1)-C(2)	1.413(5)
Ag(2)-I(1)#3	2.901(1)	C(2)-C(3)	1.357(5)
Ag(2)-I(1)	3.006(1)	C(3)-C(4)	1.403(6)
I(1)-Ag(2)#3	2.848(1)	C(4)-C(5)	1.350(5)
I(1)-Ag(2)#2	2.901(1)	C(5)-C(6)	1.361(4)
I(3)-Ag(1)#4	2.854(1)		
Angle	(°)	Angle	(°)
I(2)-Ag(1)-I(3)#1	115.29(1)	Ag(2)#2-I(1)-Ag(1)	117.02(1)
I(2)-Ag(1)-I(3)	105.84(1)	Ag(2)#3-I(1)-Ag(2)	75.11(1)
I(3)#1-Ag(1)-I(3)	105.20(1)	Ag(2)#2-I(1)-Ag(2)	74.34(1)
I(2)-Ag(1)-I(1)	116.86(1)	Ag(1)-I(1)-Ag(2)	62.20(1)
I(3)#1-Ag(1)-I(1)	111.88(1)	Ag(2)-I(2)-Ag(1)	66.60(1)
I(3)-Ag(1)-I(1)	99.53(1)	Ag(1)#4-I(3)-Ag(1)	105.20(1)

I(2)-Ag(1)-Ag(2)	56.65(1)	C(7)-S(1)-C(1)	90.50(2)
I(3)#1-Ag(1)-Ag(2)	135.30(2)	C(7)-N(1)-C(6)	114.2(3)
I(3)-Ag(1)-Ag(2)	119.42(2)	C(6)-C(1)-C(2)	119.0(3)
I(1)-Ag(1)-Ag(2)	60.43(1)	C(6)-C(1)-S(1)	112.6(2)
I(2)-Ag(2)-I(1)#2	115.93(2)	C(2)-C(1)-S(1)	128.4(3)
I(2)-Ag(2)-I(1)#3	110.32(2)	C(3)-C(2)-C(1)	117.3(4)
I(1)#2-Ag(2)-I(1)#3	105.18(1)	C(2)-C(3)-C(4)	122.1(3)
I(2)-Ag(2)-I(1)	113.92(1)	C(5)-C(4)-C(3)	120.7(3)
I(1)#2-Ag(2)-I(1)	105.95(2)	C(4)-C(5)-C(6)	118.5(3)
I(1)#3-Ag(2)-I(1)	104.60(1)	C(5)-C(6)-C(1)	122.3(3)
I(2)-Ag(2)-Ag(1)	56.75(1)	C(5)-C(6)-N(1)	128.3(3)
I(1)#2-Ag(2)-Ag(1)	135.07(2)	C(1)-C(6)-N(1)	109.5(3)
I(1)#3-Ag(2)-Ag(1)	119.06(2)	N(2)-C(7)-N(1)	120.7(3)
I(1)-Ag(2)-Ag(1)	57.38(1)	N(2)-C(7)-S(1)	126.1(2)
Ag(2)#3-I(1)-Ag(2)#2	105.18(1)	N(1)-C(7)-S(1)	113.3(2)
Ag(2)#3-I(1)-Ag(1)	104.93(1)		

Symmetry transformations used to generate equivalent atoms: #1 x-1, y, z; #2 x+1/2, -y+3/2, -z+1; #3 x-1/2, -y+3/2, -z+1; #4 x+1, y, z.

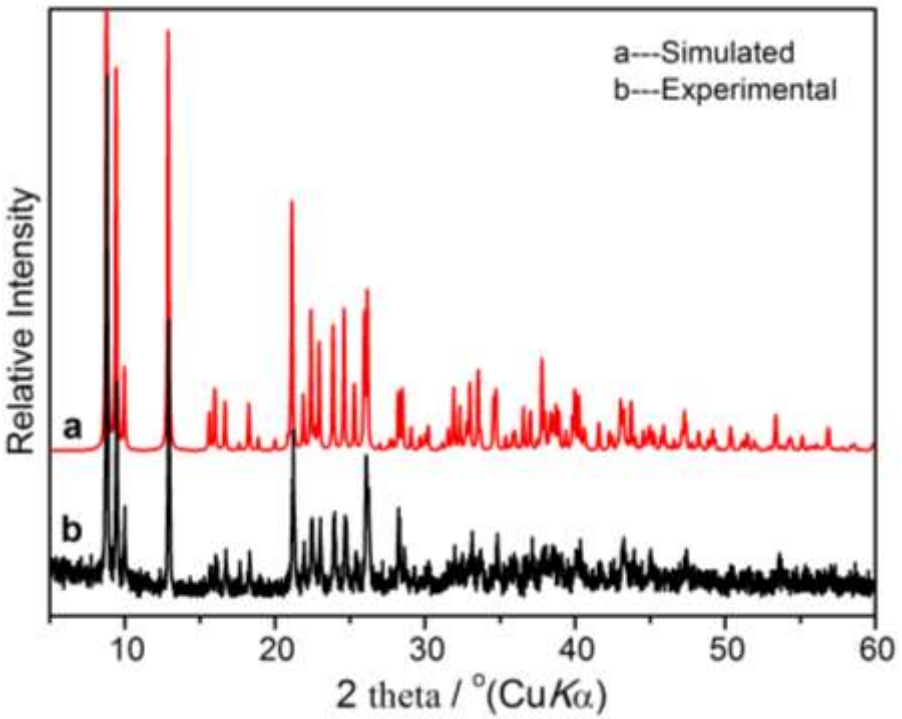
a---Simulated
b---Experimental
Relative Intensity
a
b
10
20
30
40
50
60
2 theta / °(CuKα)

(a)

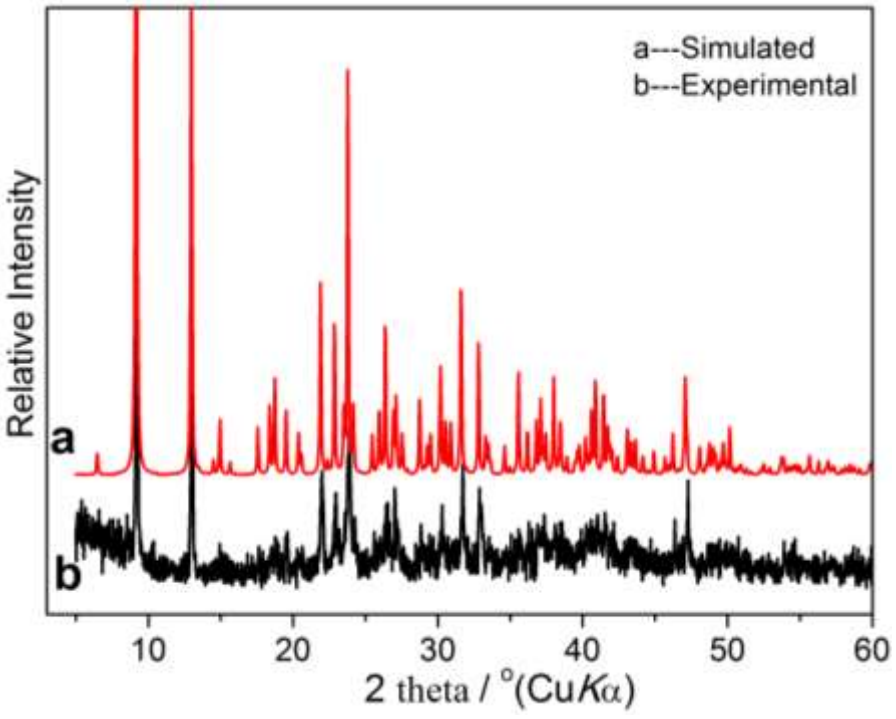
a---Simulated
b---Experimental
Relative Intensity
a
b
10
20
30
40
50
60
2 theta / °(CuKα)

(b)

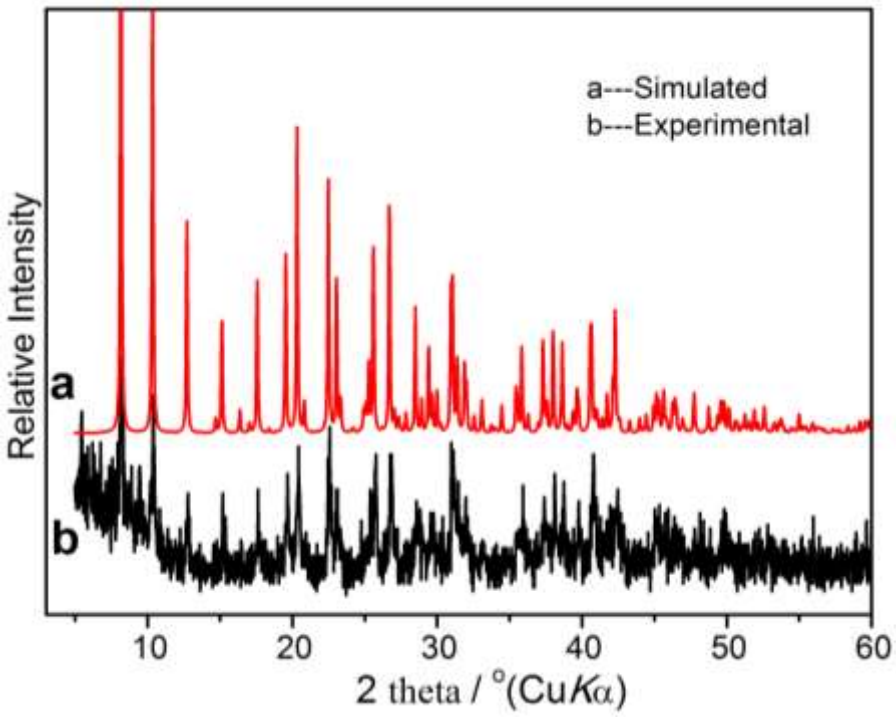

(c)

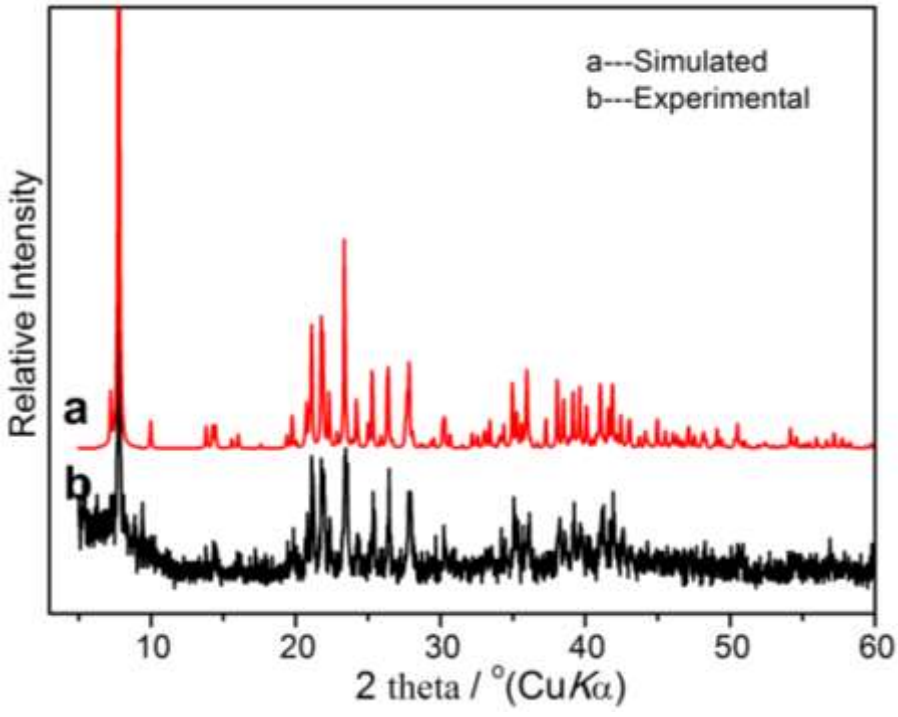

(d)

Figure S1. The PXRD patterns of **1** (a), **2** (b), **3** (c) and **4** (d) under different conditions.

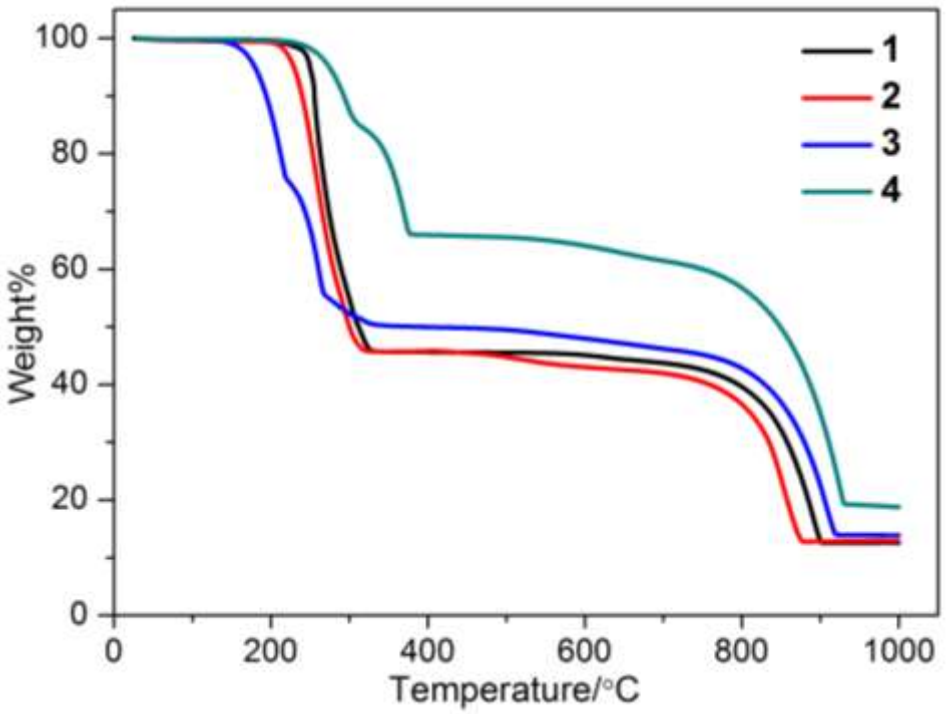

Figure S2. TGA curves of **1**–**4**.

The thermal stabilities of **1**–**4** were examined by thermogravimetric analyses (TGA) in a N_2 atmosphere from 40 to 1000 °C. The TGA curves show that compounds **1**–**4** are stable to ca. 213, 199, 134 and 210 °C, respectively, and then decomposed presumably due to the decomposition of organic components. Compounds **1**–**4** all reveal two main step weight losses before 1000 °C. For **1**, the weight loss of 54.7% between 213 and 329 °C can be attributed to the loss of one (Etbtz)I per formula (theoretical value of 55.4%). Between the temperature range 199–576 °C, compound **2** shows a weight loss of 56.4%, which may be due to the decomposition of one (Prbtz)I per formula (theoretical value of 56.5%). For **3**, the weight loss of 50.2% between 134 and 343 °C can be attributed to the loss of one (Hbtz)I per formula (theoretical value of 52.8%). Between the temperature range 210–518 °C, compound **4** shows a weight loss of 34.6%, which may be due to the decomposition of one (Etbtza)I per formula (theoretical value of 37.2%).

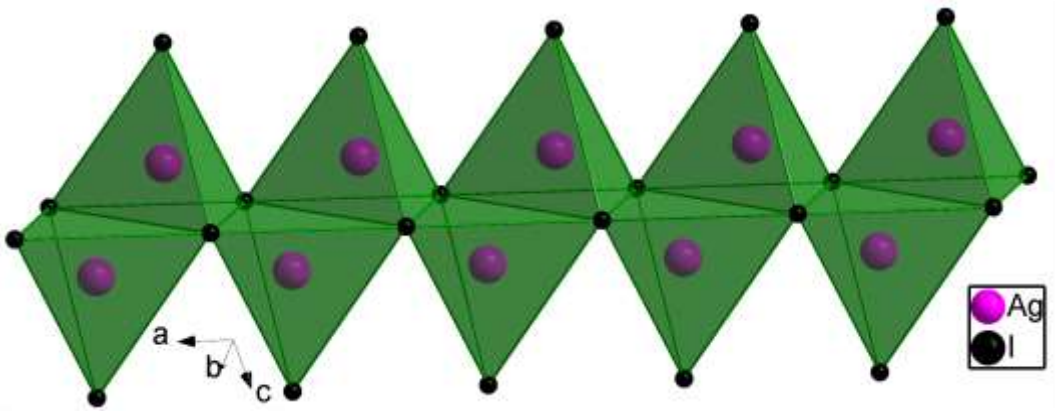

Figure S3. The β-type $(AgI_2)^-$ chain in the literature,[1] which is built up by each tetrahedral (AgI_4) unit sharing two adjacent edges with a neighbouring (AgI_4) tetrahedron.

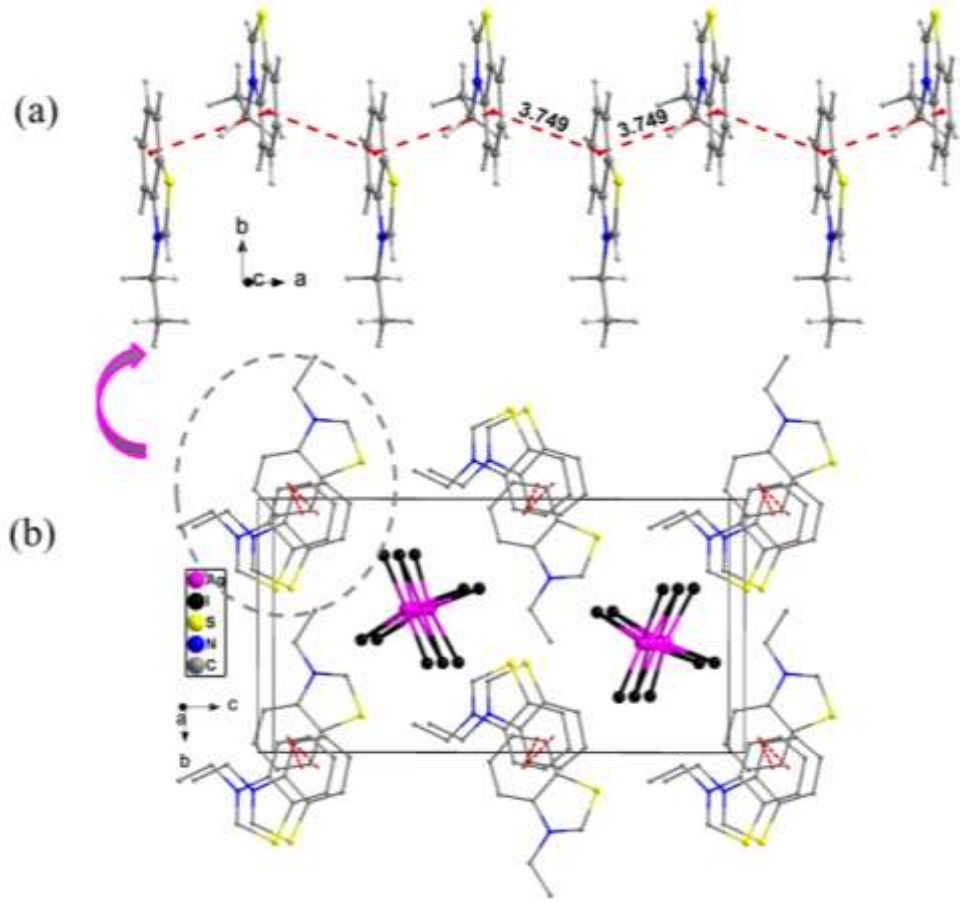

Figure S4. (a) The $(Etbtz)_n^{n+}$ cationic supramolecular chain formed by face to face π···π interactions (red dashed lines). (b) The 3-D packing diagram of **1** showing the face to face π···π interaction (red dashed lines).

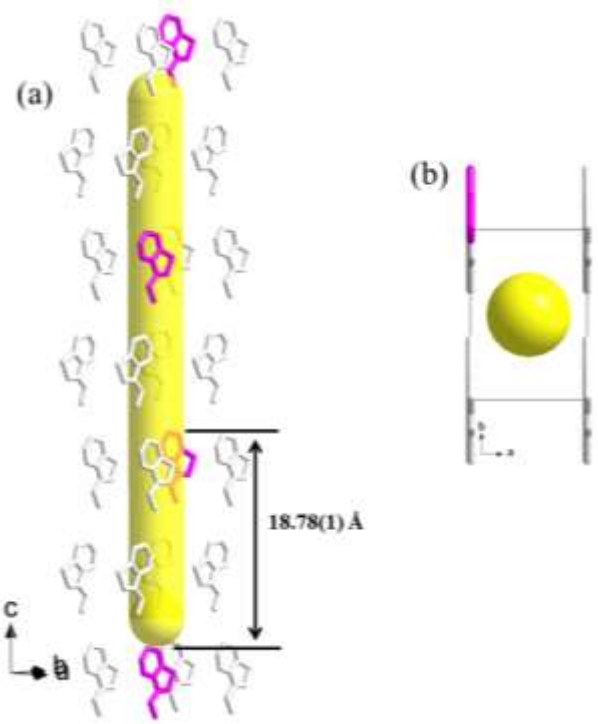

Figure S5. (a) Side view of the 2_1 helical chain of **1**. (b) View of the helical chain along the *c* direction.

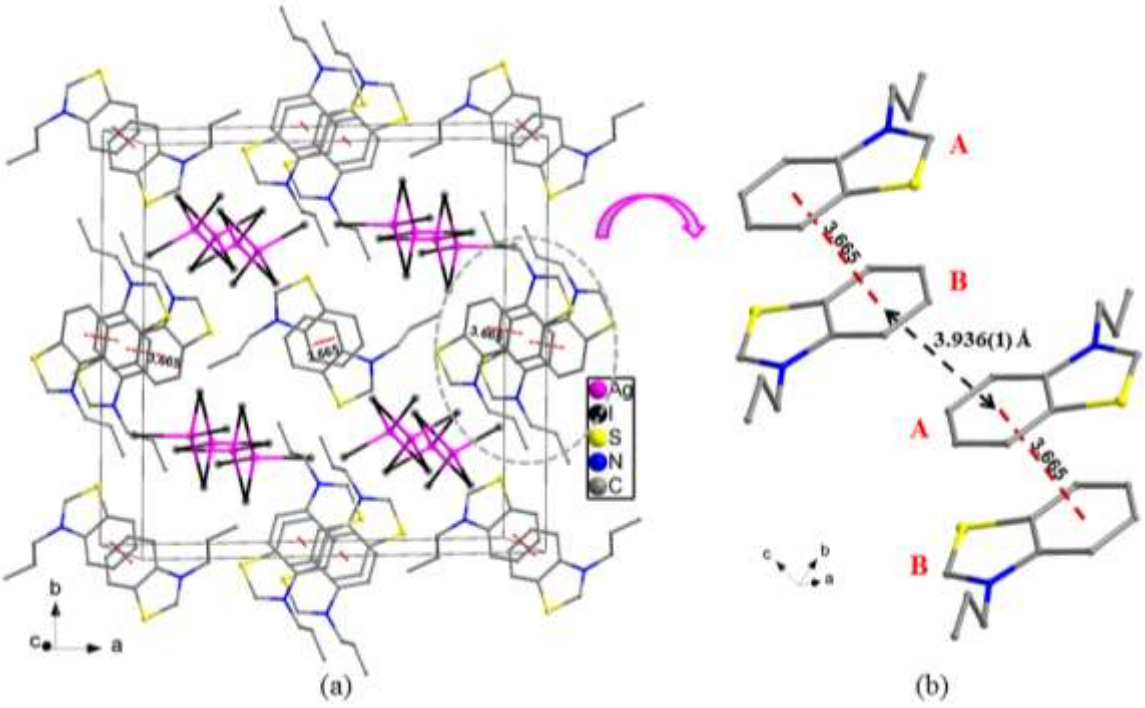

Figure S6. (a) The 3-D packing diagram of **2** showing the face to face to face π···π interaction (red dashed line). (b) The $(Prbtz)_2^{2+}$ pairs formed by face to face π···π interaction.

Table S2. Selected Hydrogen Bonds Data for **3**.

D–H···A	D–H (Å)	H···A (Å)	D···A (Å)	∠(DHA) (°)
C7-H7B···I1[a]	0.93	3.00	3.714(5)	134.3
N1-H1A···I1[b]	0.86	2.80	3.568(3)	149.7

Symmetry code: a (-1+x, y, -1+z); b (1-x, 1-y, 1-z).

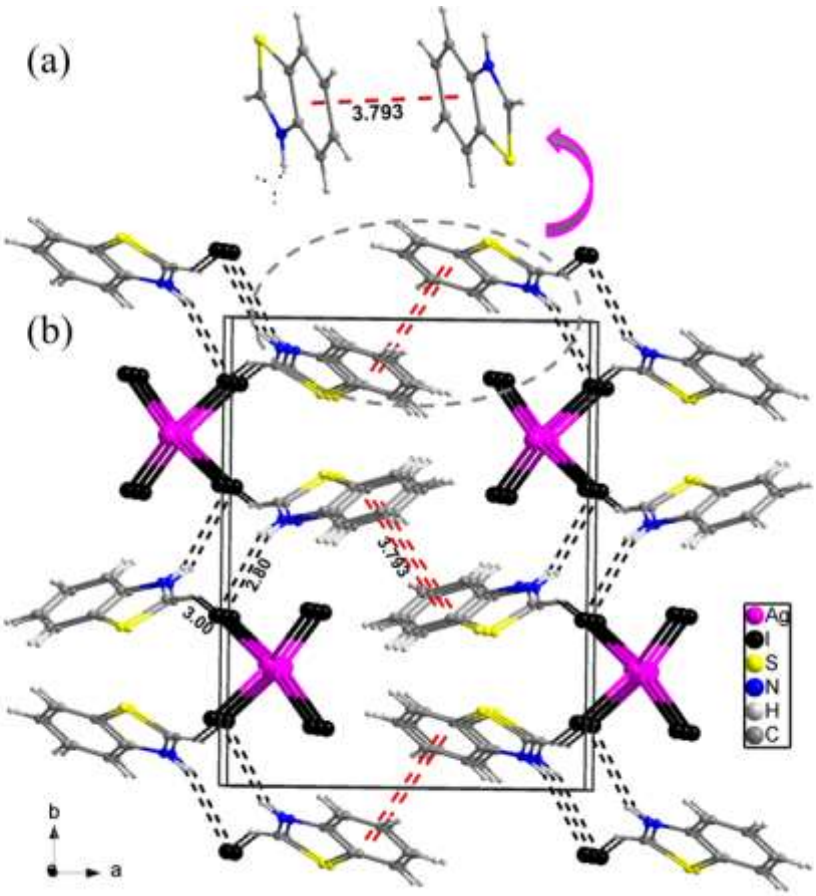

Figure S7. (a) The $(Prbtz)_2^{2+}$ pairs in **3** formed by face to face π···π interactions (red dashed lines). (b) The 3-D packing diagram showing face to face π···π interactions, C-H···I and N-H···I hydrogen bonds (black dashed lines).

Table S3. Selected Hydrogen Bonds Data for **4**.

D–H···A	D–H (Å)	H···A (Å)	D···A (Å)	∠(DHA) (°)
N1-H1A···I3[a]	0.86	2.97	3.734(3)	148.5
N2-H2B···I3[a]	0.86	2.91	3.705(4)	154.7

N2-H2C···I3[b]	0.86	2.88	3.666(4)	151.9

Symmetry code: a (x, –1+y, z); b (2-x, -1/2+y, 1/2-z).

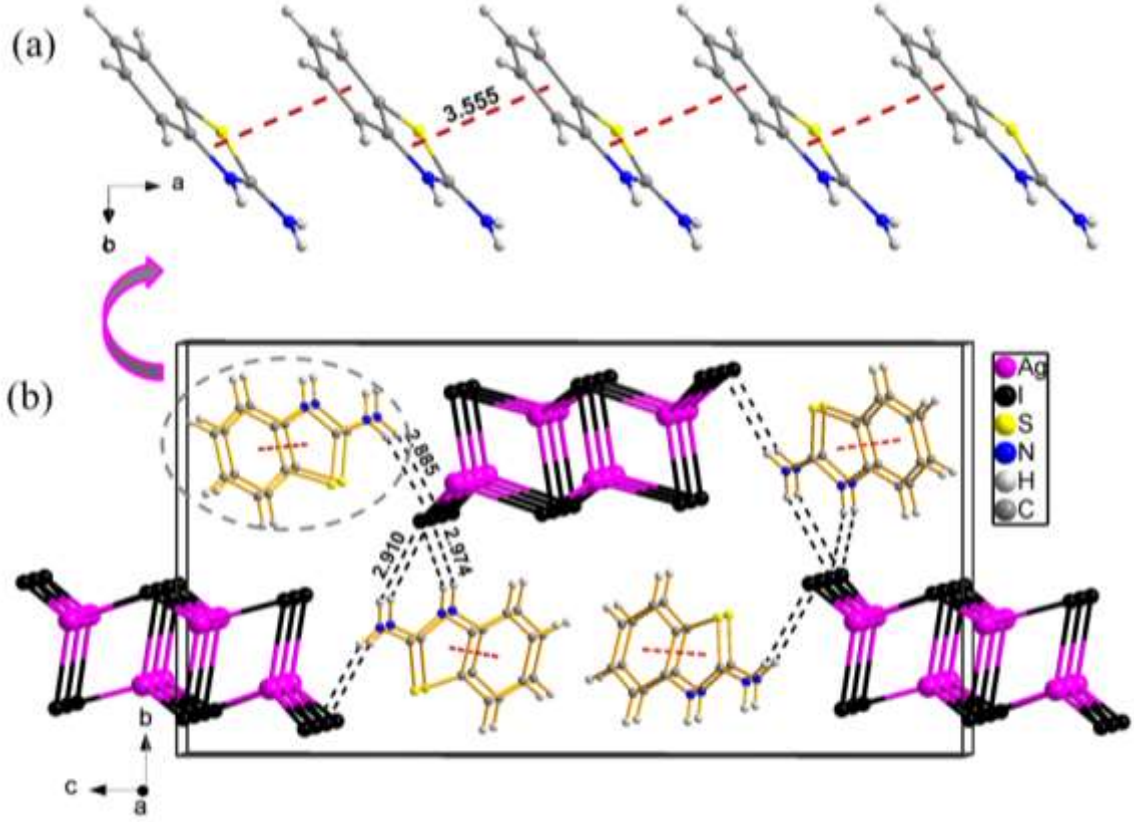

Figure S8. (a) The $(Habtz)_n^{n+}$ cationic supramolecular chain formed by face to face π···π interactions (red dashed lines). (b) The 3-D packing diagram of **4** showing face to face π···π interactions and N-H···I hydrogen bonds (black dashed lines).

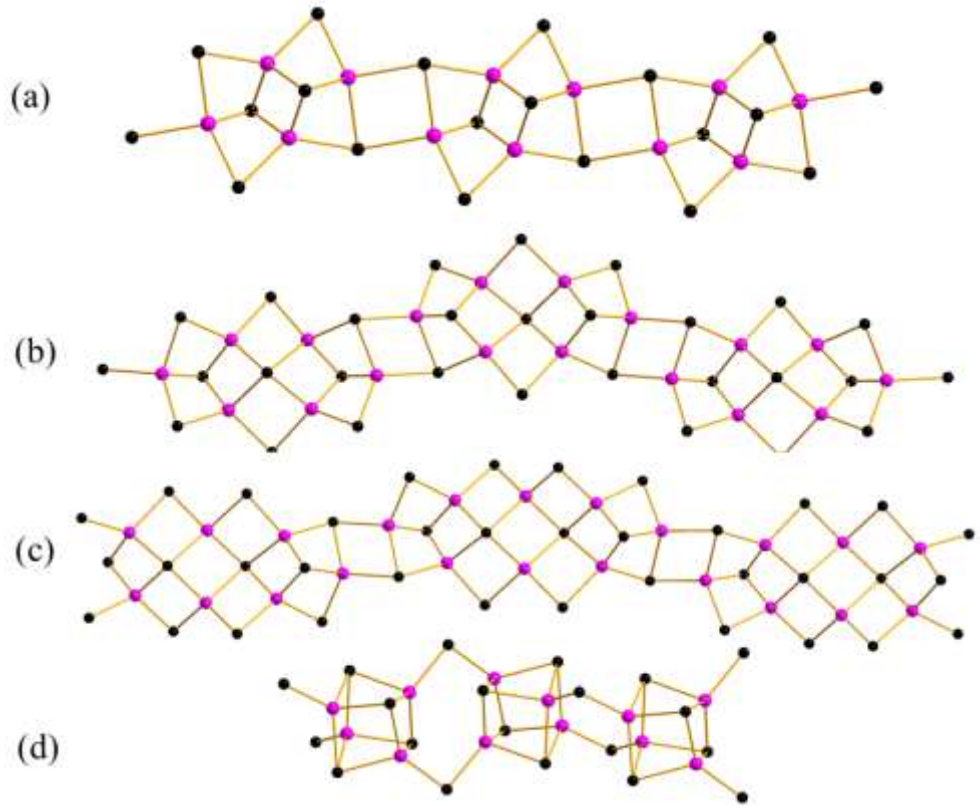

Figure S9. (a-d) The four isomers of $(Ag_2I_3)^-$ anionic chains found in reported compounds.

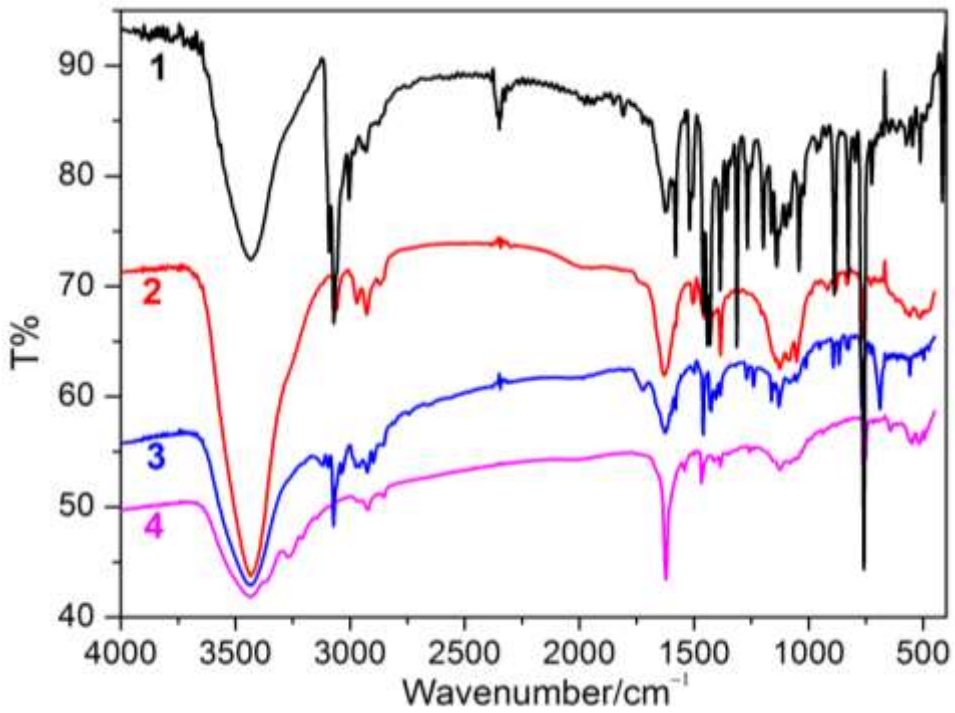

Figure S10. IR spectra of **1**–**4**.

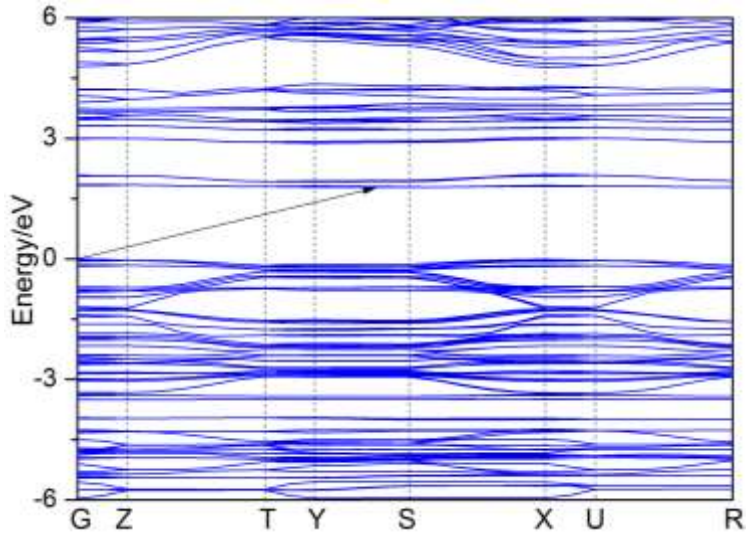
6
3
0
-3
-6
Energy/eV
G Z T Y S X U R

(a)

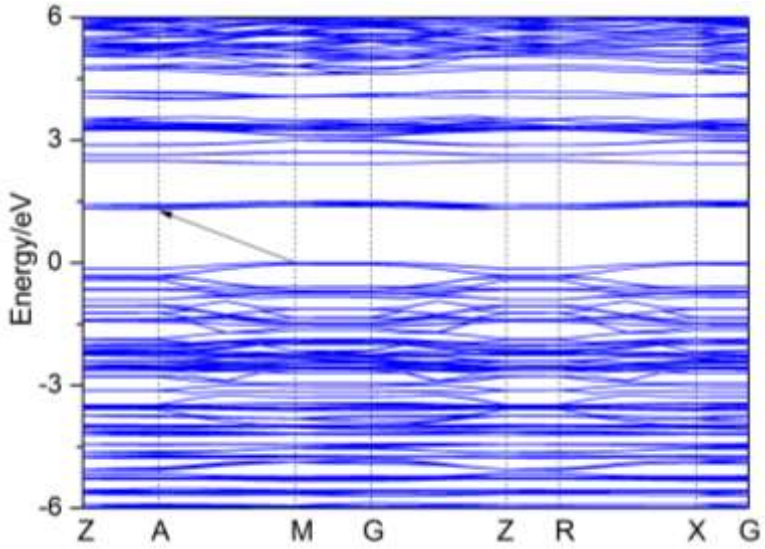
6
3
0
-3
-6
Energy/eV
Z A M G Z R X G

(b)

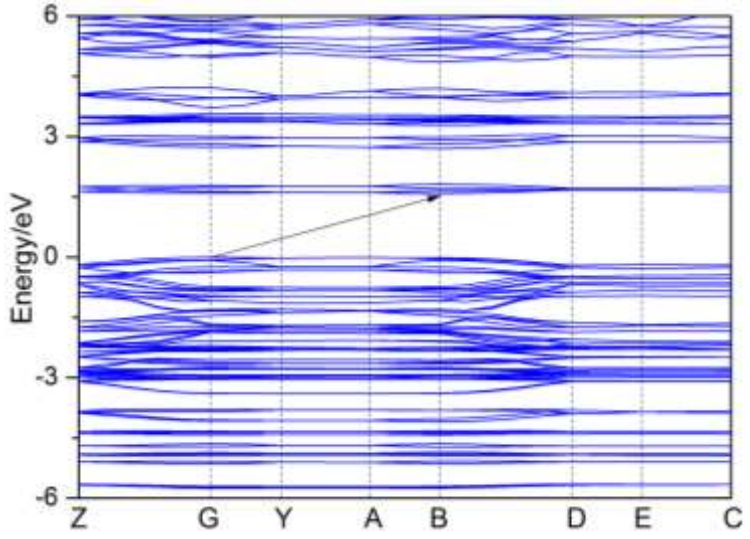
6
3
0
-3
-6
Energy/eV
Z G Y A B D E C

(c)

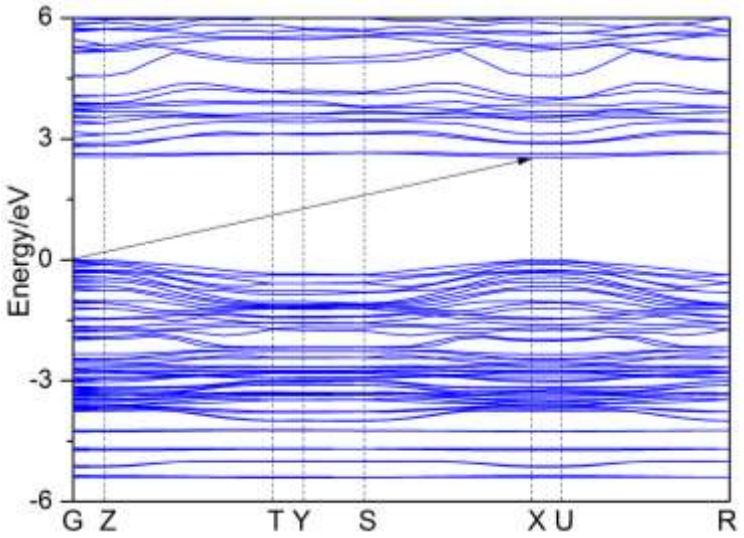

(d)

Figure S11. Band structures of **1** (a), **2** (b), **3** (c) and **4** (d). The Fermi level is set at 0 eV.

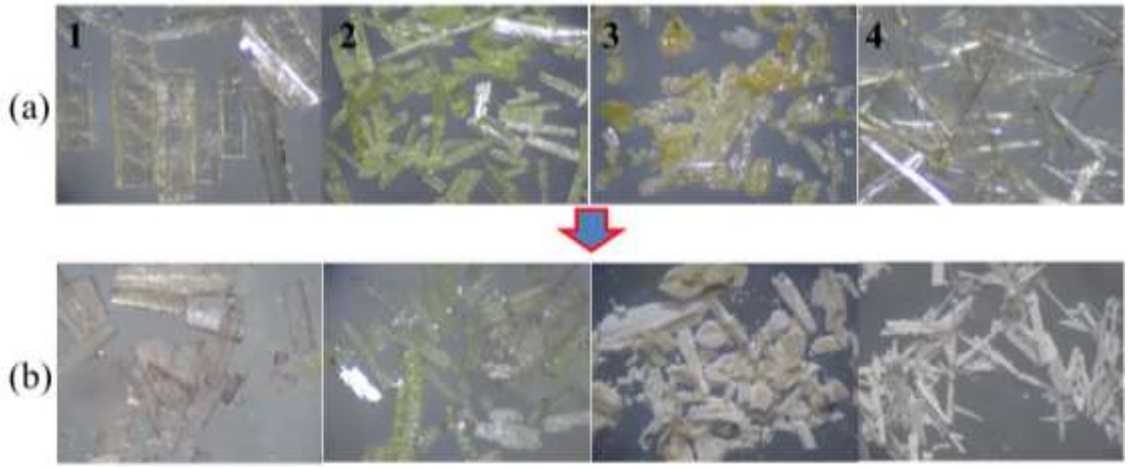

Figure S12. Photographs of the as-synthesized single crystals of **1**–**4** (a), and the crystals after being soaked in water for 1 day (b).

Table S4. Calculated Dipole Moments for Polar Units in **1**[a]

Polar unit		(AgI_4)	
Dipole moment (Deybe)	x	y	z
	0.038	–0.118	-0.070
Magnitude (Deybe)		0.142	

[a]The calculation was performed using a bond-valence approach proposed by Halasyamani et al.[2]

Photocatalytic experiments

The evaluation of photocatalytic activity of **1** for the photocatalytic decolorization of organic dye was performed at ambient temperature. The procedure was as follows: 0.020 g of powder sample was dispersed into 40 mL of Rhodamine B (RhB, 10.2 $mg \cdot L^{-1}$) aqueous solution for 30 min in the absence of light to attain adsorption-desorption equilibrium, followed by the addition of one drop of hydrogen peroxide solution (H_2O_2, 30%). A 300 W xenon arc lamp was used as a light source. An optical filter in the equipment of xenon arc lamp was used to filtering out the UV emission below 400 nm. Visible light then irradiated the above solutions. During the degradation, the mixture was stirred continuously by means of a magnetic stirrer. The test solutions were withdrawn regularly from the reactor, and dispersed powders were removed by centrifugation. At different time intervals, analytical samples were withdrawn and analyzed by UV-vis spectroscopy.

Photocatalytic degradation of organic dye of 1

Considering that **1** is stable in water and have absorption in the visible light region, it may be used as a heterogeneous photocatalyst for dye wastewater treatment, which was evaluated by the degradation of Rhodamine B (RhB) as a model dye contaminant under visible light irradiation at room temperature. For the photocatalytic degradation of RhB, the characteristic absorption of RhB at 553 nm was selected to monitor the adsorption and photocatalytic degradation process. Clearly, the change in the concentration of RhB solution is obvious when making use of **1** as a photocatalyst. **1** shows a very effective degradation of the RhB dye solution in the first 100 min, and the degradation ratios reach 94% when the light application time increases to 100 min. In the following 60 min, the degradation ratio increases very slowly and reaches 98% when the experiment was finished. For comparison, the photodegradation process of RhB without any photocatalyst has also been studied under the same condition. From Figure S14, it can be seen that when no catalyst was added to the system, the degradation of RhB was very slow, and the degradation ratio was only 8% after 100 min and finally reaches 9% after another 140 min. These results clearly indicate that **1** exhibits high photocatalytic efficiency for the degradation of RhB dye under visible light irradiation with the presence of H_2O_2.

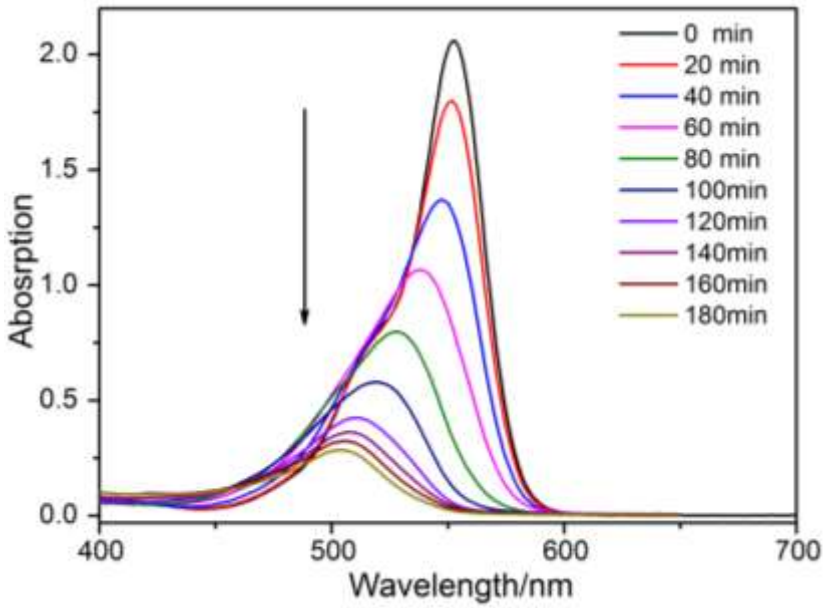

Figure S13. Time-dependent UV-vis spectra of RhB over **1**.

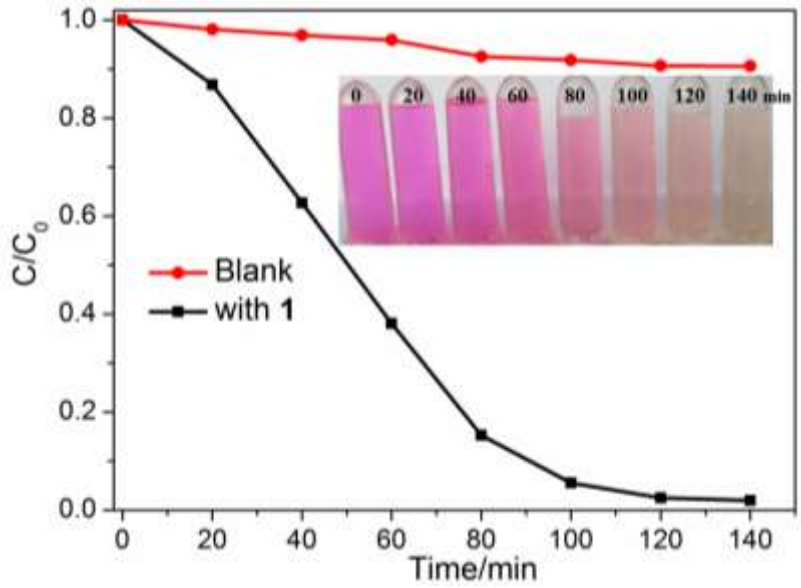

Figure S14. Time-dependent UV-vis spectra of dye solutions with or without **1**. Insert: color change photograph images of the dye solution.

Reference:

1. Liu, G. N.; Liu, L. L.; Chu, Y. N.; Sun, Y. Q.; Zhang, Z. W.; Li, C. C., *Eur. J. Inorg. Chem.* **2015**, 478-487.

2. Halasyamani, P. S., *Chem. Mater.* **2004,** *16*, 3586-3592.